Lack of Augmenter of Liver Regeneration Disrupts Cholesterol Homeostasis of Liver in Mice by Inhibiting the AMPK Pathway

Xin Wang,[1]* Ling-yue Dong,[1]* Qu-jing Gai, Wei-lun Ai, Yuan Wu, Wei-chun Xiao, Jing Zhang, and Wei An

It is well known that excessive cholesterol accumulation within hepatocytes deteriorates nonalcoholic fatty liver disease (NAFLD). Augmenter of liver regeneration (ALR) has been reported to alleviate NAFLD through anti-apoptosis; however, whether ALR could protect liver from cholesterol-induced NAFLD remains unclear. Mice with heterozygous deletion of *Gfer* (the gene for ALR, *Gfer*$^{+/-}$) were generated, and liver steatosis was induced by either choline-deficient ethionine-supplemented, methionine choline–deficient diet for 4 weeks, or high-fat diet for 16 weeks. The results showed that *Gfer*$^{+/-}$ mice developed a more severe fatty liver phenotype than *Gfer*$^{+/+}$ mice. The livers of *Gfer*$^{+/-}$ mice exhibited a higher concentration of cholesterol and low-density lipoprotein compared with the normal mice. Transcriptome-based analysis predicts low-density lipoprotein receptor (LDLR) primarily involved in the metabolic pathway. The experiments further indicate that cholesterol accumulation within hepatocytes is closely associated with enhancing the expression of LDLR and activation of sterol regulatory element binding protein 2 (SREBP2). Because adenosine monophosphate–activated protein kinase (AMPK) is a critical regulator of SREBP2 activation, we measured whether the activity of AMPK was regulated by ALR. We found that knockdown of *ALR* expression inhibited the phosphorylation of LKB1, an upstream activator of AMPK, followed by AMPK inactivation and SREBP2 maturation/nuclear translocation, leading to extensive cholesterol accumulation. Meanwhile, cellular oxidative stress increased as a result of ALR knockdown, indicating that ALR might also have a role in suppressing reactive oxygen species production. *Conclusion*: Our results confirm that ALR regulates cholesterol metabolism and alleviates hepatic steatosis probably through the LKB1-AMPK-SREBP2-LDLR pathway *in vivo* and *in vitro*, providing a putative mechanism for combating fatty liver disease. (*Hepatology Communications* 2020;4:1149-1167).

Nonalcoholic fatty liver disease (NAFLD) is becoming one of the most common chronic liver diseases worldwide. Pathologically, NAFLD can be divided into two stages: simple steatosis or steatohepatitis with hepatic inflammation and ballooning (i.e., nonalcoholic steatohepatitis [NASH]).[1] Increasing evidence suggests that a significant portion of patients with NASH may progress toward liver fibrosis and subsequently develop advanced stage liver disease, including cirrhosis, hepatic decompensation, and hepatocellular carcinoma.[2,3] The pathogenesis of NAFLD is closely correlated with all aspects of the metabolic syndrome, such as obesity, dyslipidemia and insulin resistance, complicating endpoint definitions of the disease and impeding drug intervention clinically.[4]

Although the pathogenesis of NASH is complex and incompletely understood, excessive lipid deposition in hepatocytes is now considered an essential step toward liver inflammation and hepatic toxicity.[5] In contrast to the lipotoxicity caused by triglycerides, the contribution of cholesterol to NASH development and hepatic steatosis has been inadequately defined.[6-8] A large number of investigations indicate that free cholesterol accumulation can trigger hepatic inflammation and deteriorate NASH development.[9,10] Recently, several studies reported that the lipotoxicity of free cholesterol in hepatocytes could be associated primarily with impairment on mitochondrial dynamics and biogenesis.[11,12] However, detailed mechanisms of cholesterol regulation in mitochondrial dynamics remain rather obscure.

Hepatic stimulator substance (HSS) was initially isolated from regenerating livers of rats. Partially purified HSS can stimulate the regeneration of the liver after partial hepatectomy.[13] The effect of HSS stimulation on hepatic proliferation appears to be liver-specific, but not species-specific. Intriguingly, HSS on its own did not induce proliferation of quiescent hepatocytes, but amplified the combined mitogenic effects of the epidermal growth factor and the hepatocyte growth factor. As a consequence, HSS was renamed "augmenter of liver regeneration" (ALR).[14] Nowadays, it is known that alternative splicing of the ALR gene (also known as *Gfer*) produces two proteins: a short form (sf) with 15 kDa and a long form (lf) with 22 kDa. The sf-ALR is believed to be a candidate of cytokines with a yet uncharacterized function. The lf-ALR is a sulfhydryl oxidase that resides primarily in the mitochondrial intermembrane space[15] and exerts liver protection against various types of injury, including NASH. We have demonstrated that enhancement of ALR expression in mice attenuated liver injury caused by high-fat diet or alcohol.[16,17] We also previously reported that transfection of ALR into steatotic hepatocytes could up-regulate carnitine palmitoyl transferase I (CPT1), which is propitious to the transport of long-chain fatty acid into the mitochondria.[18] Consistently, Gandhi et al. demonstrated that *ALR* liver-specific deletion in mice accelerates development of steatohepatitis and hepatocellular carcinoma.[19] They found that the association of *ALR* deletion with hepatic steatosis is partially attributed to the down-regulation of CPT1. These data clearly imply that ALR could be an important regulator for lipid metabolism in the mitochondria, and dysfunction of ALR might be related with the pathogenesis of NASH. In contrast to increasing the amount of investigations exploring the ALR combat to NASH caused by abnormal metabolism of fatty acids in the mitochondria, there is still a lack of evidence displaying cholesterol metabolism regulated by ALR and its contribution to NASH development.

ARTICLE INFORMATION:

From the Department of Cell Biology, Capital Medical University and the Municipal Key Laboratory for Liver Protection and Regulation of Regeneration, Beijing, China.

ADDRESS CORRESPONDENCE AND REPRINT REQUESTS TO:

Wei An, Ph.D.
Department of Cell Biology, Capital Medical University
10 You An Men Wai Xi Tou Tiao
100069 Beijing, China
E-mail: anwei@ccmu.edu.cn
Tel.: +86-10-83950452

Loss of hepatic cholesterol homeostasis deteriorates NASH progression. In hepatocytes, intracellular cholesterol homeostasis is controlled by a coordinate network involving cholesterol sensors and nuclear transcription factors regulating cholesterol synthesis, uptake, intracellular transport, and excretion.[20] Mature transcription factor SREBP2 is transported into the nucleus, binds to sterol regulatory elements (SRE), and activates downstream target genes such as 3-hydroxy-3-methyl-glutaryl-coenzyme A reductase (HMGCR), Niemann pick c1-like 1, and low-density lipoprotein receptor (LDLR). [3] Thus, regulation of sterol regulatory element binding protein 2 (SREBP2) is a cardinal step in maintaining cholesterol homeostasis. In this study, we aim to elucidate whether the ALR attenuating NASH could be associated with regulation of SREBP2. Moreover, we explore the potential mechanism by which SREBP2 expression is regulated. We report that inhibition of ALR expression in murine liver and hepatocytes decreased the liver kinase B1 (LKB1) phosphorylation, leading to inactivation of adenosine monophosphate–activated protein kinase (AMPK) and consequently promoting SREBP2 maturation. Activation of this signaling pathway mobilizes LDLR-mediated cholesterol transport more inward into hepatocytes, and accelerates NASH progression. In conclusion, this study unveils a pathway that explains how ALR expression attenuates NASH progression.

Materials and Methods

ANIMALS AND EXPERIMENTAL MODELS

Mice with heterozygous deletion of the *ALR* gene (designed as *Gfer*^{+/−}, C57BL/6J background) were generated as previously reported.[21] Two-month-old male *Gfer*^{+/−} mice and wild-type (WT) C57BL/6J mice were fed with standard chow or methionine choline–deficient diet (MCD) for 4 weeks, or choline-deficient, ethionine-supplemented diet (CDE, 60% high fat plus drinking water supplemented with 0.165% ethionine) for 4 weeks, or high-fat diet (HFD) for 16 weeks. The animals received humane treatment and were maintained in specific pathogen-free conditions. All of the protocols were approved in accordance with the guideline of the Ethics Committee of the Capital Medical University, Beijing, China.

MEASUREMENT OF SERUM AND HEPATIC LIPIDS

After 4 weeks of MCD or CDE diet, or 16 weeks of HFD, mice were sacrificed at termination of the experiments. The livers were collected for histological analysis, and blood samples were collected for the assay of alanine aminotransferase (ALT), aspartate aminotransferase (AST), triglyceride (TG), cholesterol (TC), high-density lipoprotein cholesterol (HDL-C), and low-density lipoprotein cholesterol (LDL-C) with an Hitachi 7600-020 clinical analyzer (Tokyo, Japan). Briefly, the liver tissues (50 mg) were homogenized for measurement of tissue lipid content of TG/TC and HDL-C/LDL-C as well using commercial kits (for TG/TC, Applygen Technologies [Beijing, China]; for HDL-C/LDL-C, Jiancheng Bioengineering Institute [Nanjing, China]).

RNA SEQUENCING AND DATA ANALYSIS

Total RNA was isolated from the livers of *Gfer*^{+/−} mice or *Gfer*^{+/+} mice fed the CDE diet with TRIzol (Invitrogen, Carlsbad, CA) and then sequenced by Illumina Xten sequencing (San Diego, CA). The analysis of RNA sequence (RNA-seq) was performed as previously described.[18] The Kyoto Encyclopedia of Gene and Genomes (KEGG) pathway analysis was used for enrichment analysis of different expressed genes. The expressed genes with a corrected *P* value of less than 0.05 were considered significantly different and being enriched. All data analyses were performed in the R statistical environment (version 3.5.1).

CELL CULTURE

HepG2 cells were obtained from the American Type Culture Collection (Manassas, VA). The stable *ALR*-knockdown (sh*ALR*) and *ALR*-overexpression (*ALR*-Tx) cells were established as described previously.[22] Cells were cultured with Dulbecco's modified Eagle's medium (DMEM) supplemented with

10% fetal bovine serum in an incubator with 5% CO_2 at 37°C. Primary hepatocytes were isolated from the livers of 2-month-old $Gfer^{+/-}$ and WT mice,[23] and maintained in hepatocyte medium (ScienCell, Carlsbad, CA). To induce hepatocyte steatosis, cells were cultured in sterol depletion medium (DMEM supplemented with 10% lipoprotein-deficient serum [LPDS]), 5 μm simvastatin, and 10 μm mevalonic acid for 24 hours.[24]

For primary hepatocytes of $Gfer^{+/-}$ mice, cells were transfected with adenoviral vector containing the *ALR* gene (Adv-*ALR*) or control Adv vector for 48 hours. Meanwhile, the Adv-*ALR* bearing green fluorescent protein was used to calibrate the transfection efficiency.

LDL UPTAKE ASSAY

Cells were washed three times with phosphate-buffered solution (PBS) and incubated with 5 μg/mL DiI-labeled LDL or 0.5% bovine serum albumin (BSA) as a control at 37°C for 1 hour. Then, cells were washed three times with ice-cold PBS supplemented with 0.5% BSA and fixed by 4% paraformaldehyde and analyzed by confocal microscope (TCS-NT SP8; Leica, Wetzlar, Germany). The relative fluorescence signal of every single cell was quantified by Image-Pro Plus (Media Cybernetics, Rockville, MD). Fluorescence in control cells was set to 100%.

QUANTITATIVE REAL-TIME PCR AND WESTERN BLOTTING

Total RNA was isolated from liver tissue or cultured cells using the RNeasy mini-kit (QIAGEN, Maryland) and reverse-transcribed into complementary DNA for quantitative real-time PCR assay as described previously.[22]

To visualize the expressions of cholesterol-related proteins, western blotting was used, and the primary antibodies against LDLR (diluted 1:1000; Abcam, Cambridge, United Kingdom), SREBP2 (diluted 1:2,000; Abcam), AMPK (diluted 1:1,000), phosphorylated AMPK (diluted 1:1,000; Abcam), ALR (diluted 1:1,000; Proteintech, Chicago, IL), phosphorylated LKB1 (diluted 1:500, Cell Signaling Technology, Beverly, MA), LKB1 (diluted 1:800, Abcam), SREBP1c (diluted 1:1,000; Abcam), and

goat anti-rabbit secondary antibody (diluted 1:5,000; Proteintech) were used.

TISSUE STAINING AND HISTOLOGY

For staining, 5-μm-thick liver tissue slices were sectioned and stained with hematoxylin and eosin or Oil Red O. The hepatic histology was observed by light microscopy DM500 B (Leica Microsystems, Wetzlar, Germany).

For LDLR staining, liver sections (5 μm) were incubated with anti-LDLR primary antibody at 1:200 in 3% BSA dissolved in PBS at 4°C for overnight. After three washes with PBS, liver sections were incubated with goat anti-rabbit immunoglobulin G (IgG) secondary antibody at 1:200 with 3% BSA for 30 minutes. Quantitative results were calculated by Image-Pro Plus software to average the percentage of LDLR-positive area for five fields in each section.

For immunofluorescence, cells were plated at a density of 2×10^5 cells per confocal dish. After 24 hours of LPDS treatment, cells were fixed with 4% paraformaldehyde and incubated with anti-LDLR primary antibody (1:200) at 4°C overnight. After staining with Alexa Fluor 488 goat anti-rabbit IgG secondary antibody (1:200), fluorescence images were viewed and captured by laser confocal microscopy (Leica).

CHROMATIN IMMUNOPRECIPITATION ASSAY

Mouse monoclonal anti-SREBP2 antibody (Santa Cruz Biotech, Dallas, TX) was used for immunoprecipitation assay. The following PCR primers were used: human LDLR-SRE forward, 5′-GGGACCCAAATA CAACAAATCAAGT-3′; reverse, 5′-TG AGGTTT CTAGCAGGGGGAGG-3′; mouse LDLR-SRE forward, 5′-TCAGGGGTT AAAAGAGACGATG-3′; reverse, 5′-CCAGTACTAGGGGCGAGGTTT-3′. Ultimately, a 188-bp (human) or 129-bp (mouse) fragment containing a SRE sequence of LDLR promoter was obtained.

ATP ASSAY

A Cell Titer-Glo luminescent cell viability assay kit (Promega, Madison, WI) was used for the

detection of intracellular ATP content. After centrifugation, the supernatant of cells or homogenized tissues were mixed with the reaction reagent for 10 minutes, and measured by a Glomax 96 Microplate Luminometer (Promega) following the manufacturer's instructions.

SEAHORSE XF ASSAY

HepG2 cells (1 × 10^5 cells/well) were plated in a Seahorse XFp culture microplate (Seahorse Bioscience, Santa Clara, CA). The measurement of oxygen consumption rate (OCR) was as previously described.[25] HepG2 cells were stimulated with 0.25 μm carbonyl cyanide 4-(tri-fluoromethoxy) phenylhydrazone and 10 μm oligomycin (Seahorse Bioscience). Data of OCR were recorded using the Seahorse Metabolism Analyzer (Seahorse XFp).

FLOW CYTOMETRY

Reactive oxygen species (ROS) induced by LPDS in hepatocytes can be detected by flow cytometry. Cells (5 × 10^5) were seeded in 6-well plates. After stimulation, dichloro-dihydro-fluorescein diacetate was added to cells and incubated for 30 minutes in the dark at 37°C. Fluorescence measurement was performed as previously described.[26]

ROS STAINING

For ROS staining, 5-μm-thick frozen liver tissue slices were sectioned and stained with ROS staining solution (Sevicebio Technology, Wuhan, China) at 37°C in the dark for 30 minutes. After washing three times with PBS, the nucleus was counterstained with 4′,6-diamidino-2-phenylindole for 10 minutes. Quantitative results were calculated by Image-Pro Plus software to average the percentage of ROS-positive area for three fields in each section.

MEASUREMENT OF MALONDIALDEHYDE

The liver tissues (50 mg) were homogenized for measurement of tissue malondialdehyde (MDA) content as well using commercial kits (Applygen Technologies).

STATISTICAL ANALYSIS

Experimental results are presented as the mean ± SD. Comparisons between the two groups were performed with GraphPad Prism 7 software (San Diego, CA). Student t test was used to determine the statistical significances between the two groups. Bonferroni correction was used to adjust the significance the levels for differences among more than two groups in which $P < 0.05$ was considered statistically significant.

Results

INHIBITION OF ALR DETERIORATED HEPATIC CHOLESTEROL ACCUMULATION IN MICE WITH CDE OR MCD DIET

Heterozygous knockout (KO) of *Gfer* resulted in a remarkable reduction of hepatic ALR expression (Fig. 1A). As shown in Fig. 1B, the MCD and CDE diets actually cause weight loss in mice, but the weight of CDE-fed mice decreased at the first week and then increased again, and still lower than that of chow diet group mice at the fourth week. Nevertheless, the ratio of liver/body weight showed no significant difference between *Gfer*$^{+/-}$ and *Gfer*$^{+/+}$ mice after CDE or MCD for 4 weeks (Fig. 1C). However, the hepatic steatosis was more pronounced in *Gfer*$^{+/-}$ mice than that in *Gfer*$^{+/+}$ mice (Fig. 1D,E). Although liver function tests such as serum ALT and AST showed no significant differences between the *Gfer*$^{+/-}$ and *Gfer*$^{+/+}$ mice (Fig. 1F,G), the severity of hepatic steatosis based on NAFLD scoring[27] and inflammation in *Gfer*$^{+/-}$ mice was significantly higher than in *Gfer*$^{+/+}$ mice (Table 1). It is worth noting that, after the MCD and CDE diet for 4 weeks, the amounts of serum TC and LDL-C were significantly reduced in *Gfer*$^{+/-}$ mice as compared with the WT mice, whereas hepatic cholesterol deposition in *Gfer*$^{+/-}$ mice was significantly higher in both CDE and MCD animals (Table 2). Taken together, these results suggest that liver steatosis generated by administering the CDE or MCD is more severe in *Gfer*$^{+/-}$ mice and could be partially a result of dysregulation of cholesterol homeostasis.
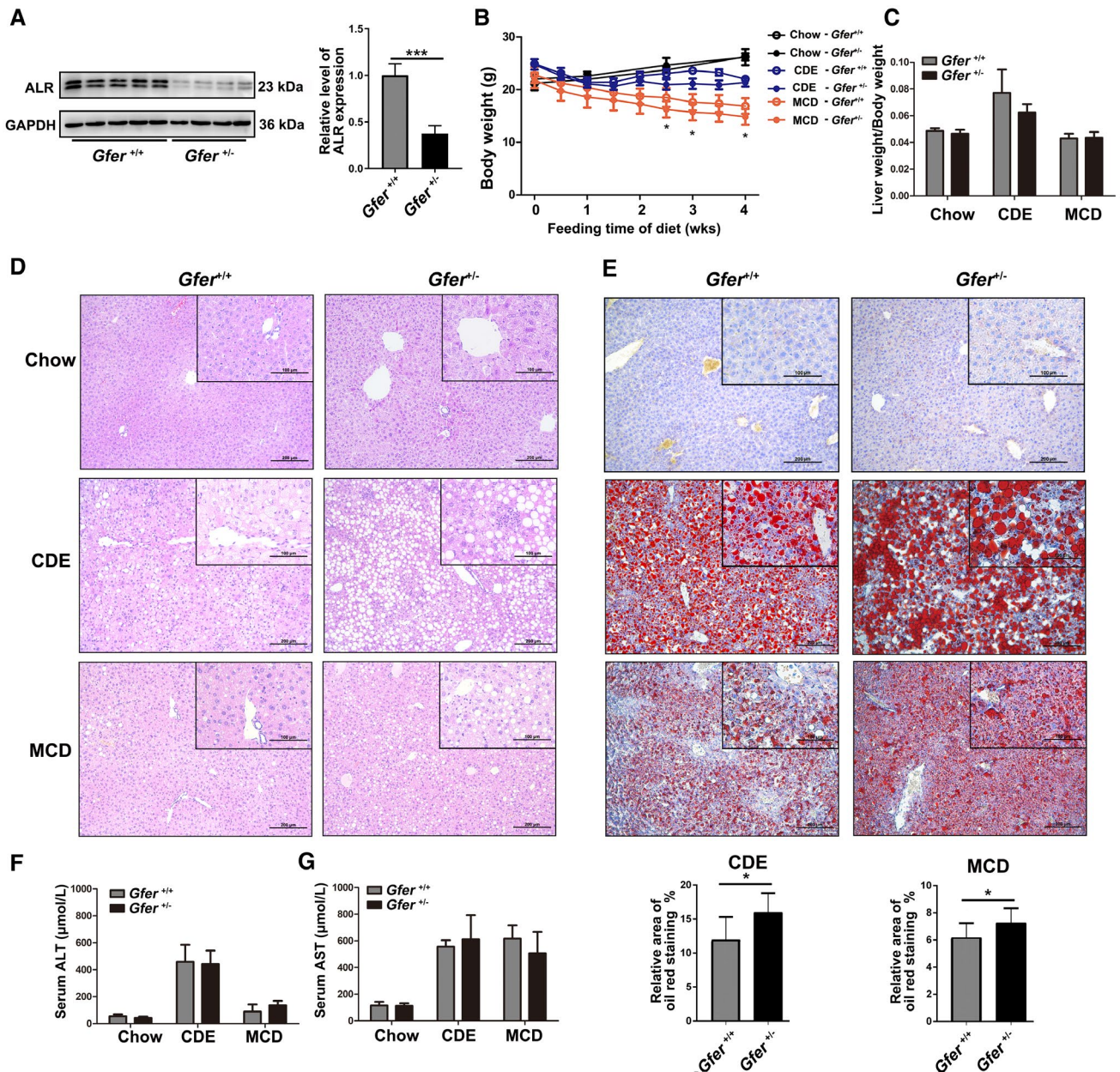
FIG. 1. Inhibition of ALR-deteriorated hepatic lipid accumulation in CDE or MCD diet. (A) Western blot Analysis of ALR protein levels in $Gfer^{+/+}$ and $Gfer^{+/-}$ mice liver tissues ($Gfer^{+/+}$ mice, n = 5; $Gfer^{+/-}$ mice, n = 4). The experiment was repeated at least three times. (B) Fluctuation curves of mouse body weights. The body weight was recorded every 3 days. "*" represents $Gfer^{+/+}$ mice versus $Gfer^{+/-}$ mice fed with MCD diet, $P < 0.05$. (C) Comparison of liver weight/body weight between $Gfer^{+/+}$ and $Gfer^{+/-}$ mice after CDE or MCD diet (chow diet, n = 3 mice per group; CDE diet, n = 6 mice per group; and MCD diet, n = 10 mice per group). (D) Hematoxylin and eosin staining of mouse liver tissue (chow diet, n = 3 mice per group; CDE diet, n = 6 $Gfer^{+/+}$ mice and n = 8 $Gfer^{+/-}$ mice; and MCD diet, n = 7 mice per group). Scale bars: 200 μm and 100 μm. (E) Oil Red O staining revealed the condition of liver lipid accumulation, and the results were quantified five images/mouse by Image-Pro Plus (n = 6 mice per group). Scale bars: 200 μm and 100 μm. (F,G) Mouse serum ALT and AST levels were measured to evaluate liver function (chow diet, n = 3 mice per group; CDE diet, n = 6 $Gfer^{+/+}$ mice and n = 8 $Gfer^{+/-}$ mice; and MCD diet, n = 7 mice per group). In (A), (B), and (E), data are expressed as the mean ± SD. *$P < 0.05$, ***$P < 0.0001$.

TABLE 1. EFFECTS OF ALR ON LIVER INJURY AFTER 4 WEEKS OF CDE OR MCD DIET

Parameters	4-Week CDE Diet		4-Week MCD Diet	
	$Gfer^{+/+}$ (n = 5)	$Gfer^{+/-}$ (n = 8)	$Gfer^{+/+}$ (n = 7)	$Gfer^{+/-}$ (n = 7)
Inflammation	0.76 ± 0.51	1.42 ± 0.53*	0.89 ± 0.53	0.99 ± 0.49*
Steatosis	2.08 ± 0.09	2.69 ± 0.21*	1.21 ± 0.39	2.29 ± 0.81*

Note: Liver damage is evaluated by inflammation and steatosis score.
*$P < 0.05$ versus $Gfer^{+/+}$.

TABLE 2. LIPID PROFILE OF SERUM AND LIVERS OF MICE AFTER CDE OR MCD DIET FOR 4 WEEKS

	Parameters	4-Week CDE diet		4-Week MCD diet	
		$Gfer^{+/+}$ (n = 7)	$Gfer^{+/-}$ (n = 7)	$Gfer^{+/+}$ (n = 7)	$Gfer^{+/-}$ (n = 7)
Serum	TG (mmol/L)	0.99 ± 0.09	1.407 ± 0.23	0.65 ± 0.7	0.53 ± 0.08*
	TC (mmol/L)	2.35 ± 1.01	1.62 ± 0.4*	1.76 ± 0.29	1.48 ± 0.27†
	HDL-C (mmol/L)	1.02 ± 0.52	1.19 ± 0.54	0.9 ± 0.44	0.71 ± 0.29
	LDL-C (mmol/L)	0.56 ± 0.13	0.17 ± 0.07†	0.1 ± 0.04	0.067 ± 0.04*
Liver	TG (µmol/g pr)	496.6 ± 433.6	760.4 ± 467.5	94.26 ± 97.32	186.99 ± 75.81*
	TC (µmol/g pr)	55.18 ± 24.82	88.25 ± 23.0†	39.74 ± 9.0	51.96 ± 9.49*
	HDL-C (mmol/g PR)	44.18 ± 23.26	36.57 ± 14.2	0.23 ± 0.24	0.39 ± 0.33
	LDL-C (mmol/g PR)	1.69 ± 0.48	2.14 ± 0.47†	0.64 ± 0.12	0.9 ± 0.25*

Note: The TC, TC, HDL-C, and LDL-C levels were measured in serum and liver tissue.
*$P < 0.05$.
†$P < 0.01$ versus $Gfer^{+/+}$.

ASSOCIATION OF LIVER STEATOSIS WITH IMPAIRMENT ON CHOLESTEROL UPTAKE BY LDLR IN *ALR*-DEFICIENT MICE

To predict the possible mechanism associated with hepatic cholesterol deposition during NAFLD in $Gfer^{+/-}$ mice, liver tissues from CDE $Gfer^{+/-}$ and $Gfer^{+/+}$ mice were taken, and whole genome transcriptome analysis was conducted by using RNA-seq (Fig. 2A). A total of 1,088 genes were detected and expressed differentially, including 610 up-regulated genes and 478 down-regulated genes with fold changes of 1.5 or higher in $Gfer^{+/-}$ mice compared with the $Gfer^{+/+}$ mice (Fig. 2B). All of the differentially expressed genes were analyzed by KEGG enrichment analysis, and approximately 20 pathways with the greatest significance in $Gfer^{+/-}$ mice compared with $Gfer^{+/+}$ mice are summarized in Fig. 2C. Most of the significant pathways were related to complement and coagulation, focal adhesion, extracellular matrix–receptor interaction, indicating that *ALR* knockdown may affect cell migration. Interestingly, we noticed that pathways of cholesterol-related

metabolism were significantly enriched between $Gfer^{+/-}$ and $Gfer^{+/+}$ mice. In particular, in the up-regulated gene panel, two important genes, HMGCR and LDLR, which regulate cholesterol synthesis and uptake, were overexpressed (Fig. 2D). Accordingly, messenger RNA (mRNA) expressions of these two genes were measured and revealed that hepatic *Ldlr* mRNA of $Gfer^{+/-}$ mice increased by two-fold as compared with $Gfer^{+/+}$ mice after the CDE diet, and increased by about 50% in $Gfer^{+/-}$ mice in comparison to the WT littermates subjected to MCD (Fig. 2E). Likely, *Hmgcr* mRNA was also elevated more than two-fold in $Gfer^{+/-}$ mice compared with $Gfer^{+/+}$ mice subjected to the CDE diet; however, no significant variation was observed in the MCD mice (Fig. 2F). The expression of ATP-binding cassette (ABC) transporters such as *Abcg5*, *Abcg8*, and *Abca1* and cytochrome P450 enzymes for bile acid synthesis (*Cyp7a1* and *Cyp27a1*) were not altered (Fig. 2G). Increased expression of *Ldlr* and *Hmgcr* genes, to a large extent, explains cholesterol deposition by ALR depletion. Consistent with *Ldlr* mRNA, LDLR protein levels were also increased as shown by western blot (Fig. 3A) and immunohistochemistry in $Gfer^{+/-}$ mice (Fig. 3B).

In accordance with hepatic cholesterol accumulation in livers of Gfer$^{+/-}$ mice, the cellular cholesterol contents were significantly increased in *ALR*-deficient cells (Supporting Fig. S3). Therefore, our research focuses on ALR regulation on LDLR in hepatic steatosis.

As shown in Fig. 4A, the cellular uptake of DiI-LDL was remarkably enhanced to approximately 1.5-4.0-fold higher in short hairpin RNA (shRNA)-*ALR*-HepG2 cells, and *ALR*-deficient primary hepatocytes isolated from Gfer$^{+/-}$ livers. Meanwhile,
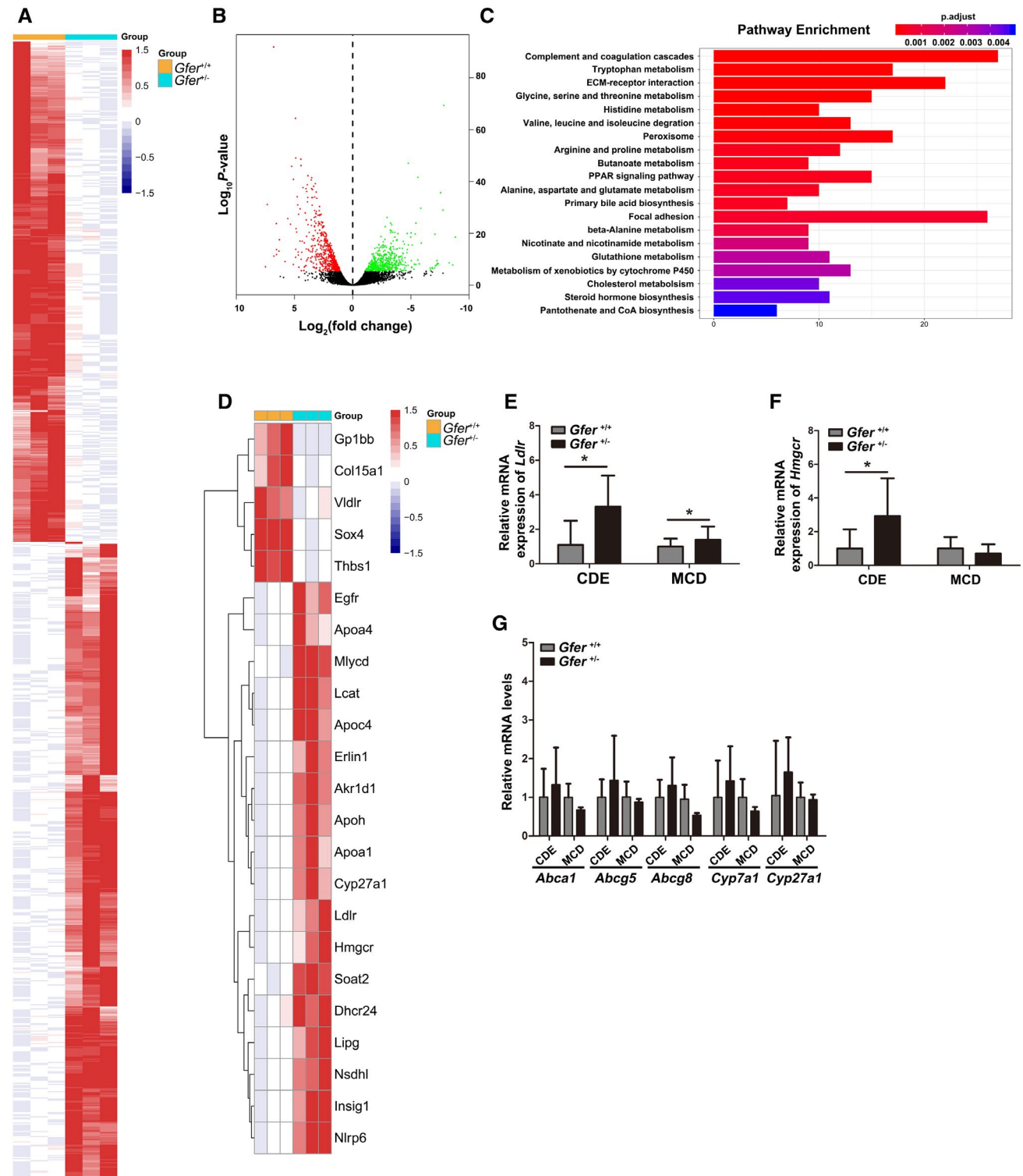
FIG. 2. Comparative transcriptome analysis of livers in *Gfer*$^{+/+}$ and *Gfer*$^{+/-}$ mice fed the CDE diet. (A) Heat maps of differentially expressed genes in CDE-diet *Gfer*$^{+/-}$ mice compared with *Gfer*$^{+/+}$ mice (n = 3 mice per group). (B) Comparative transcriptome analysis using RNA-seq. Genes that were expressed greater than or equal to a 1.5-fold change are highlighted in red (higher) or green (lower). (C) KEGG pathway analyses were carried out by differentially expressed genes. (D) Heat maps of the differentially expressed genes that encode extracellular matrix–receptor interaction, and cholesterol metabolism–associated molecules. (E) Heterozygous deletion of ALR increased the *Ldlr* mRNA level in *Gfer*$^{+/-}$ mice after CDE or MCD diet (CDE diet, n = 8 *Gfer*$^{+/+}$ mice and n = 12 *Gfer*$^{+/-}$ mice; and MCD diet, n = 7 mice per group). (F,G) Hepatic mRNA levels of cholesterol synthesis, efflux, and degradation-related genes were analyzed by quantitative PCR (CDE diet, n = 8 *Gfer*$^{+/+}$ mice and n = 12 *Gfer*$^{+/-}$ mice; and MCD diet, n = 7 mice per group). In (E)-(G), data are expressed as the mean ± SD for three independent experiments. *P < 0.05. Abbreviations: ECM, extracellular matrix; PPAR, peroxisome proliferator-activated receptor.
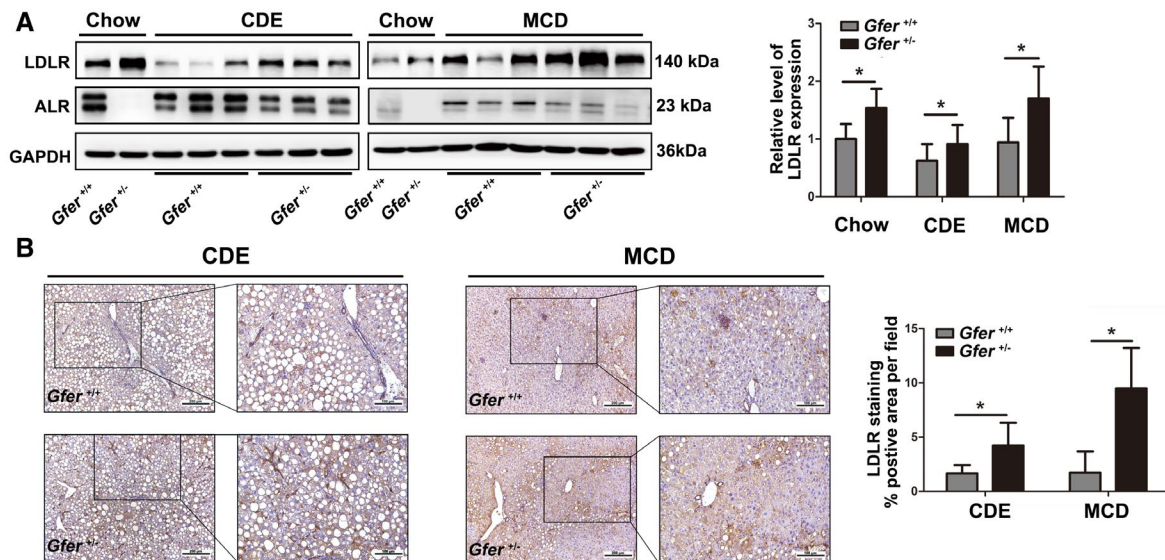
FIG. 3. Enhancement of LDLR expression when the expression of ALR was inhibited *in vivo*. (A) Analysis of *LDLR* expression level with western blot (CDE diet, n = 5 *Gfer*$^{+/+}$ mice and n = 8 *Gfer*$^{+/-}$ mice; and MCD diet, n = 7 mice per group). (B) Deficiency of ALR enhanced the location and expression of LDLR, and results were quantified five images/mouse by Image-Pro Plus (n = 5 mice per group). Scale bars: 200 μm and 100 μm. In (A) and (B), data are expressed as the mean ± SD for three independent experiments. *P < 0.05. Abbreviation: GAPDH, glyceraldehyde 3-phosphate dehydrogenase.

Ldlr mRNA levels and protein expression were also drastically elevated in *ALR*-deficient cells (Fig. 4B-D). Based on these data, we speculate that enhanced cholesterol uptake into hepatocytes through LDLR might be attributed to partial *ALR* knockdown and could definitively aggravate hepatic steatosis.

ENHANCEMENT OF LDLR EXPRESSION IS ASSOCIATED WITH SREBP2 MATURATION

LDLR-mediated cholesterol transport is closely regulated by two different transcription factors. One of them, SREBP2, following activation, can up-regulate the expression of genes dealt with cholesterol uptake. [28] Thus, the protein levels of SREBP2 were measured. As shown in Fig. 5, mature SREBP2 (SREBP2-M) was significantly elevated in livers of *Gfer*$^{+/-}$ mice compared with those of *Gfer*$^{+/+}$ mice. Similarly, down-regulation of ALR also enhanced SREBP2 maturation and translocation into nucleus following sterol depletion (Fig. 5B,C). The chromatin immunoprecipitation assay verified that the nuclear-translocated SREBP2 could bind with *LDLR* promoter DNA extracted either from liver tissue or from cultured cells, and this binding increased prominently in the *Gfer*$^{+/-}$ livers or *ALR*-lacking hepatocytes (Fig. 5D,E), implying that down-regulation of *ALR* could potentially promote *Ldlr* transcription, thereby favoring LDL uptake into hepatocytes.
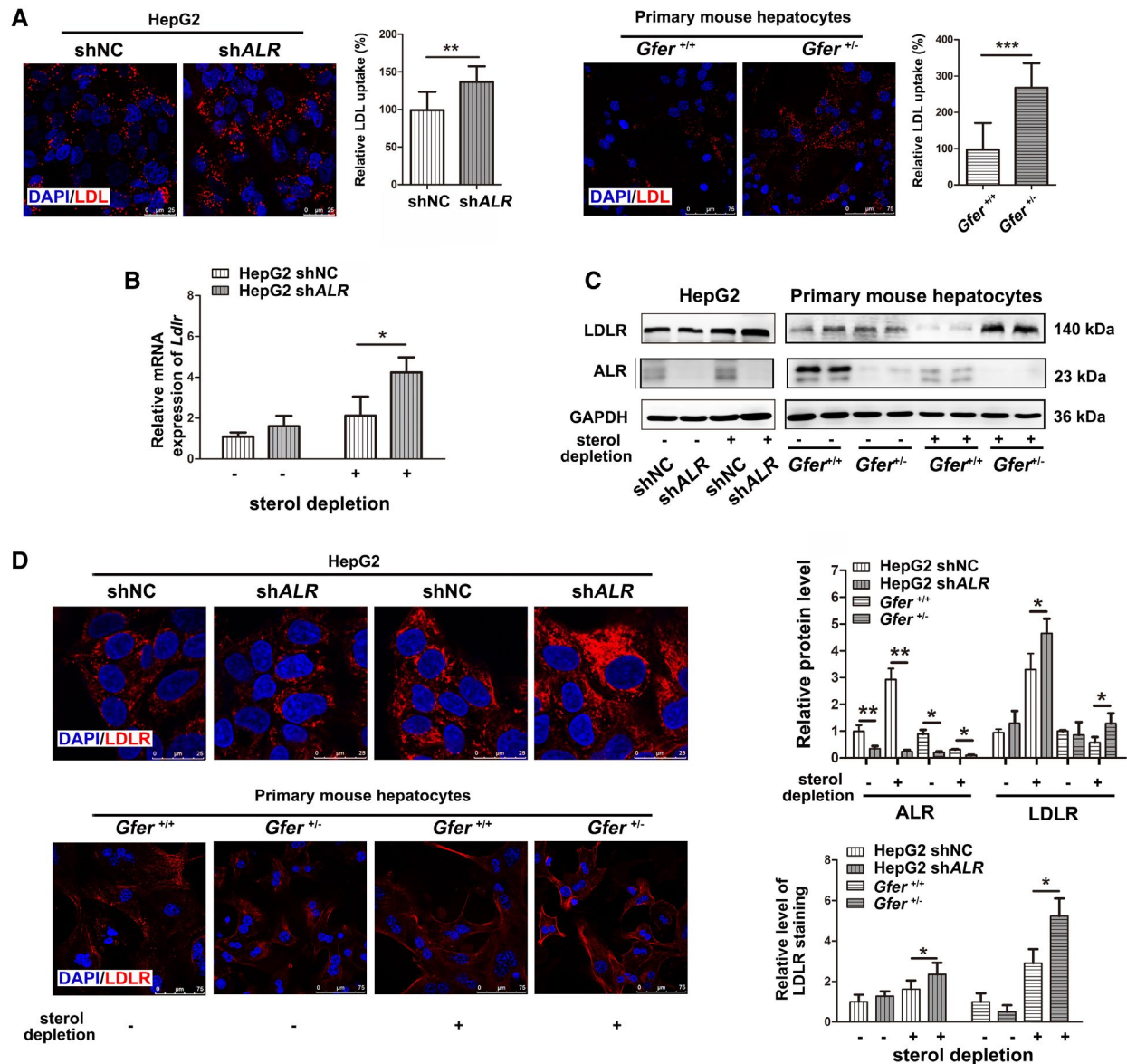
FIG. 4. Enhancement of LDLR expression by down-regulation of ALR *in vitro*. (A) After LPDS treatment, cells were incubated with DiI-labeled LDL and then observed by confocal microscopy. Relative fluorescence signal of every single cell was quantified by Image-Pro Plus. Fluorescence in control cells was set to 100%. Scale bars: 25 μm and 75 μm. (B) After LPDS treatment, HepG2 cells were lysed to detect the *Ldlr* mRNA level. (C,D) The expression and location of LDLR in HepG2 cells and primary mouse hepatocytes were inhibited when reducing the expression of ALR. The relative fluorescence signal was quantified at least seven images at each group by Image-Pro Plus. Scale bars: 25 μm and 75 μm. In (A)-(D), data are expressed as the mean ± SD for three independent experiments with three multiple holes in each repetition. *$P < 0.05$, **$P < 0.01$, ***$P < 0.001$. Abbreviation: DAPI, 4′,6-diamidino-2-phenylindole; shNC, scramble shRNA.

REGULATION OF SREBP2 BY AMPK IN *ALR*-DEFICIENT CELLS

It is known that SREBP maturation is regulated by AMPK phosphorylation. Phosphorylated AMPK restricts the SREBP2 to nuclear translocation.[29]

As indicated in Fig. 6A, AMPK phosphorylation at Thr172 was effectively inhibited in liver tissue of $Gfer^{+/-}$ mice after CDE or MCD diet. Meanwhile, phosphorylated AMPK^{Thr172} (p-AMPK^{Thr172}) was significantly reduced in *ALR*-shRNA HepG2 and in primary hepatocytes of $Gfer^{+/-}$ mice in sterol-depletion
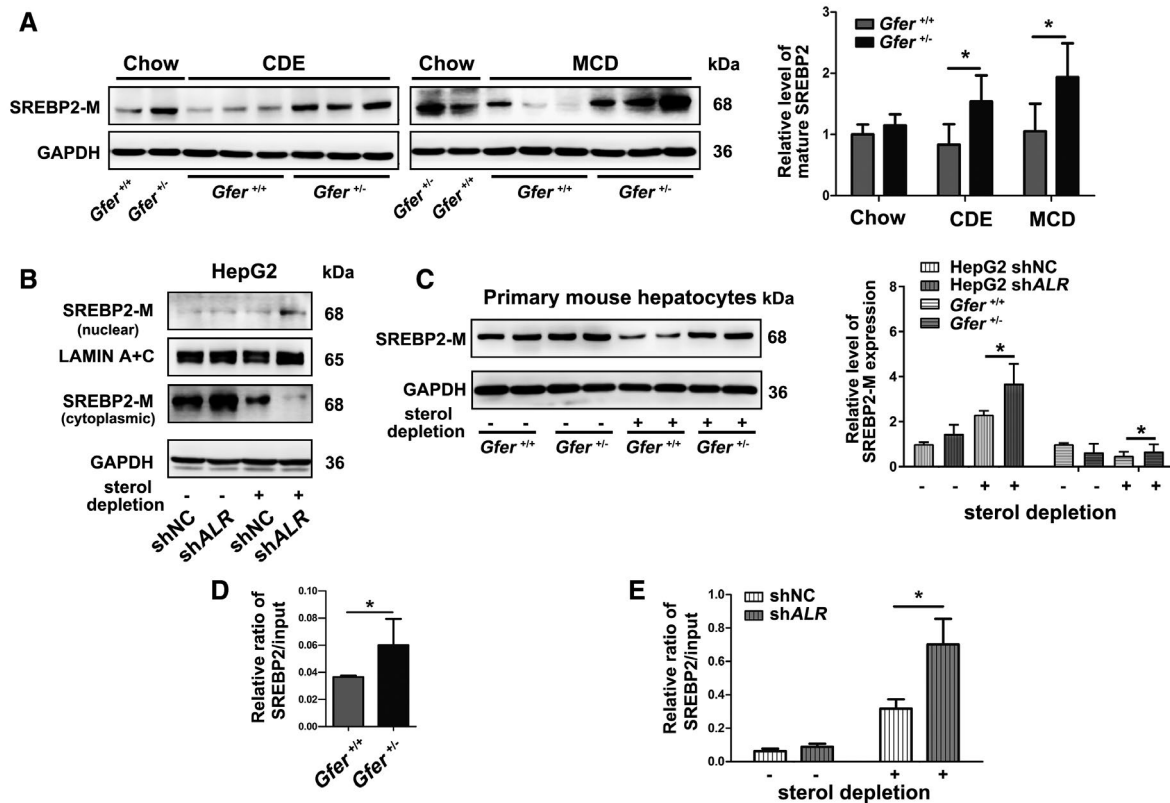
FIG. 5. Enhancement of LDLR expression is associated with SREBP2 maturation. (A) The effect of ALR on SREBP2-M level *in vivo* was analyzed by western blot analysis (Chow diet, n = 5 mice per group, CDE diet, *Gfer*^+/+ n = 5 mice, *Gfer*^+/- n = 8 mice, MCD diet, n = 7 mice per group). (B), (C) SREBP2-M and its target gene LDLR protein levels in HepG2 cells and primary mouse hepatocytes were analyzed by western blot. (D), (E) Chromatin immunoprecipitation analysis of livers taken from mice after feeding CDE diet for 4 weeks (n = 2 mice per group) and HepG2 cells after LPDS-treatment. The promoter region containing the SREBP2 binding site was analyzed by qPCR. In A-E, data were mean ± SD for three independent experiments.*P < 0.05. Abbreviation: ChIP, chromatin immunoprecipitation.

status (Fig. 6B). A769662, a potent activaor of AMPKα catalytic subunit, could concentration-dependently activate the phosphorylation AMPK-Thr172. Meanwhile, SREBP2 maturation and LDLR expression were dominantly inhibited (Fig. 6C), resulting in a gradual decrease in cellular LDL uptake (Fig. 6D).

It is also noted that the hepatic or serum levels of TC and TG were significantly increased in *Gfer*^+/- mice as compared with *Gfer*^+/+ mice after HFD for 16 weeks (Fig. 7B,C). The expression levels of different proteins were also consistent with the results of CDE and MCD diets (Fig. 7D). Additionally, regulation of AMPK-SREBP2-LDLR provided by ALR was analyzed with western blot, of which the phosphorylation of AMPK presents a pattern apparently identical to that exhibited in CDE/MCD mice for 4 weeks.

Surprisingly, rescue experiments indicated that if the *ALR* gene was re-introduced into *ALR*-deficient primary hepatocytes (Fig. 8A, right panel), the AMPK^Thr172 phosphorylation appeared elevated again; at the same time, the LDL uptake decreased by up to 75% of the control (Fig. 8B,C). These results indicate that the regulation of ALR on SREBP2 and subsequent impact on LDL uptake are probably dependent on phosphorylation of AMPK at residue Thr172.

DOWN-REGULATION OF ALR-IMPAIRED MITOCHONDRIAL FUNCTION

In patients with NAFLD, hepatic AMPK activity and ATP synthesis significantly decreased.[30,31] Next, we questioned whether *ALR* deletion could affect mitochondrial ATP synthesis and function as well. As
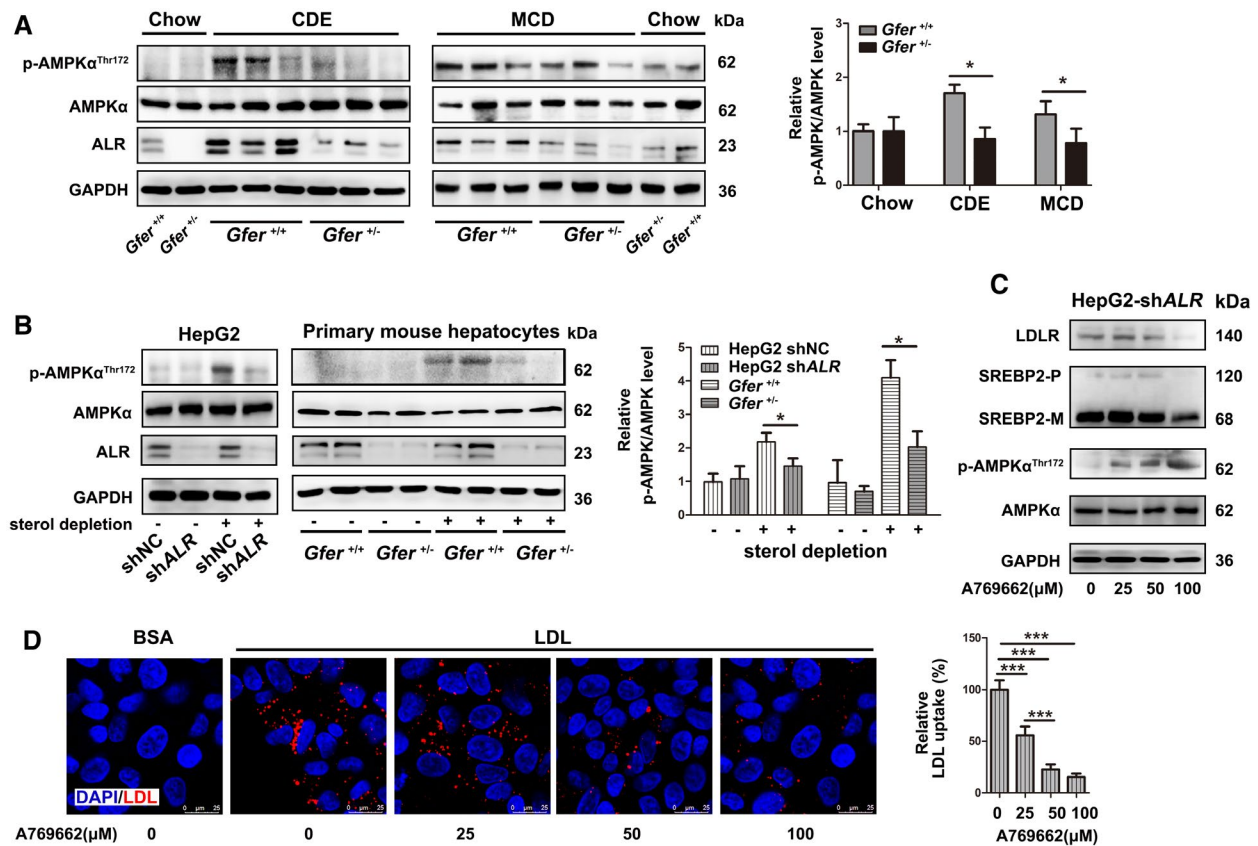
FIG. 6. Regulation of SREBP2 controlled by AMPK in *ALR*-deficient cells. (A,B) Western blot analysis was performed to detect the level of phosphorylated AMPK level in CDE/MCD diet mice (n = 5 mice per group) or HepG2 cells and primary mouse hepatocytes. (C) HepG2-sh*ALR* cells were treated with various doses of A769662 (0, 25, 50, and 100 μm) for 24 hours accompanied by sterol depletion medium, and the p-AMPK, SREBP2-M, and LDLR protein levels were measured by western blot analysis. (D) After A769662 and LPDS treatment stimulation, HepG2-sh*ALR* cells were incubated with 5 μg/mL DiI-labeled LDL or 0.5% BSA as a control at 37°C for 1 hour, and finally imaged by confocal microscopy. Scale bars: 25 μm. In (A)-(D), data are expressed as the mean ± SD for three independent experiments. Meanwhile, each cell experiment was equipped with three multiple holes in each repetition. *$P < 0.05$, ***$P < 0.001$.

shown in Fig. 9A, *ALR* knockdown in HepG2 cells inhibited the use of oxygen for oxidative phosphorylation, as indexed by OCR. As a result, hepatic ATP contents decreased significantly in partially *ALR*-deficient mice (Fig. 9B). It is known that AMPK is an essential enzyme that regulates cellular energy homeostasis. The activity of AMPK is regulated by a rational ratio of (AMP) ADP/ATP and its upstream kinase LKB1 as well. Thus, LKB1 activity was measured in *ALR*-lacking cells to estimate whether ALR might be a putative regulator on LKB1. As shown in Fig. 9C,D, the hepatic LKB1 phosphorylation at Ser 426 was greatly inhibited in *Gfer*$^{+/-}$ mice. To elucidate whether a decrease in ATP synthesis exerts a regulatory impact on AMPK activity by suppressing LKB1 phosphorylation in hepatocytes, HepG2 cells were simultaneously treated with oleic acid (200 μm) and oligomycin A (an inhibitor of ATP synthase), ATP synthesis and LKB1 phosphorylation were measured. As indicated in Supporting Fig. S4A,B, these stimuli could dose-dependently inhibit cellular ATP production and LKB1 phosphorylation. To this end, we conclude that the lack of *ALR* could affect the LKB1-AMPK-SREBP2 pathway to promote hepatic cholesterol accumulation by enhancing LDL uptake.

DOWN-REGULATION OF ALR INCREASES THE LEVEL OF ROS AND PROMOTES SREBP2 MATURATION

It is known that ROS can activate SREBP2 directly.[32] In our study, we found that a decrease
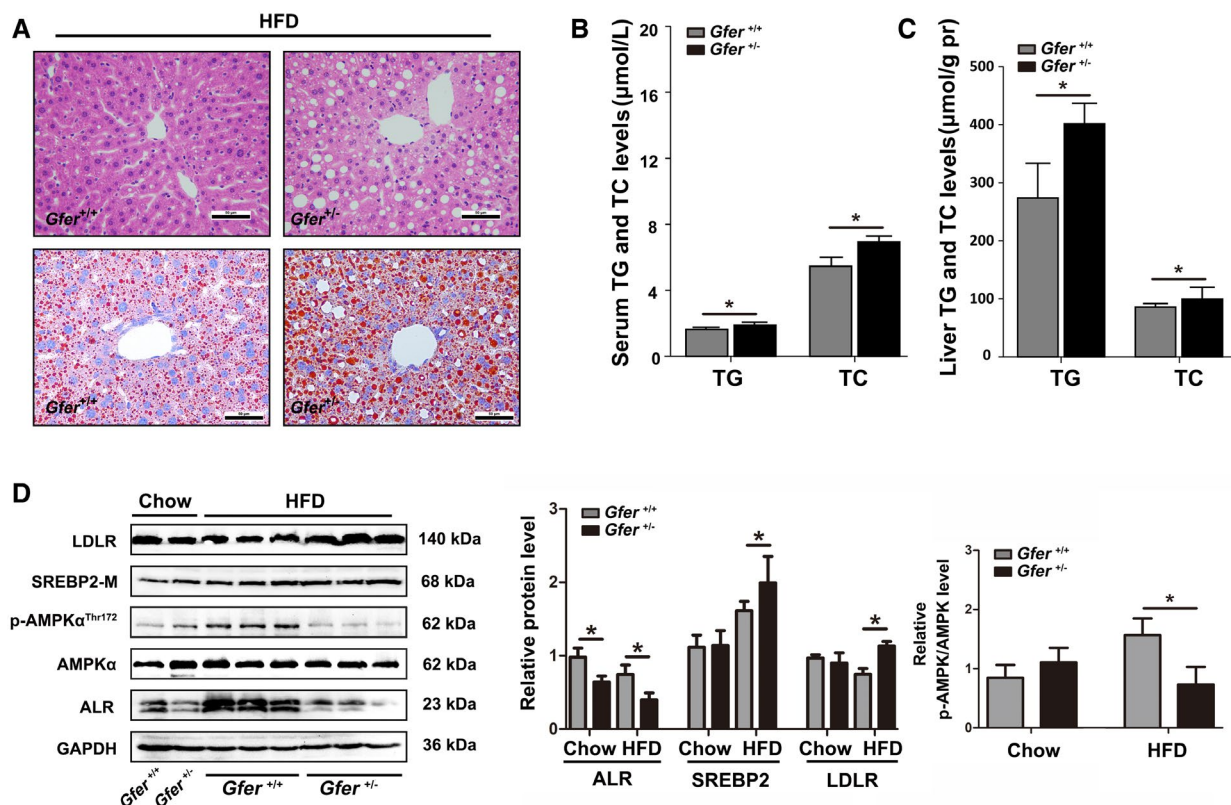
FIG. 7. Partial ALR deletion deteriorated hepatic steatosis and interfered the phosphorylation of LKB1-AMPK proteins in livers of mice suffering from 16-week HFD. (A) Hematoxylin and eosin staining and Oil Red O staining of liver tissue of HFD mice (n = 5 mice per group). Scale bars: 50 μm. (B,C) TG and TC contents in serum and liver tissue were measured (n = 5 mice per group). (D) Western blot analysis was performed to detect the level of LDLR, SREBP2-M, phosphorylated AMPK, and AMPK levels in HFD mice (n = 5 mice per group).

in the expression of ALR could elevate the levels of hepatic ROS or MDA (Fig. 10A,B). Treatment of *ALR*-shRNA HepG2 cells with antioxidant/reductant (N-acetylcysteine, NAC) reduced the cellular ROS level (Fig. 10C) and restored the cellular ATP contents to a certain degree (Fig. 10D). Next, we sought to verify the role of ROS in SREBP2 maturation. For this purpose, we directly measured the protein level and found significant reduction in the SREBP2-M and piAMPK level in the NAC pretreatment group (Fig. 10E). These data suggest that increasing the production of ROS could destroy the intracellular cholesterol homeostasis through SREBP2, and this process may be AMPK-independent.

Discussion

In this study, we show that the partial inhibition of ALR causes reduced activation of AMPK, which

in turn causes up-regulation of SREBP2-mediated LDLR expression, leading to increased cholesterol uptake into hepatocytes. Several studies have indicated that ALR could protect the liver against NAFLD injury through the regulation of lipid metabolism in mice.[16,19,33] Our previous study has shown that ALR could preserve mitochondrial CPT1 activity, which assists the transport of long fatty acids into mitochondria for β-oxidation,[19,34] and as a result, facilitates the clearance of excessive hepatic lipids during the development of NASH.[19] ALR-L-KO (liver-specific depletion of ALR) mice develop extensive steatosis at the age of 2 weeks, which could be related to inhibition of the expression and activity of CPT1 in the livers and impaired fatty acid β-oxidation.[16] Furthermore, a recent report shows that cellular ALR increases the expression of fatty acid binding protein 1, which binds toxic free fatty acids, promoting mitochondrial β-oxidation by elevating CPT1.[33] These
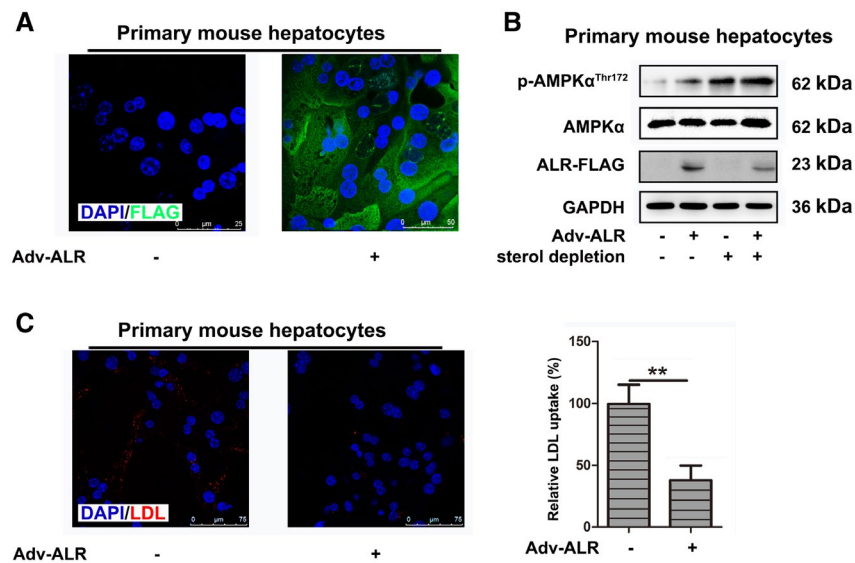
FIG. 8. Up-regulation of ALR can reduce cholesterol accumulation. (A) After being isolated from $Gfer^{+/-}$ mice and incubated for 24 hours, primary hepatocytes were transfected with adenoviral-ALR or viral vector for 48 hours. The immunofluorescence assay was conducted to demonstrate the effect of adenoviral ALR-flag transfection. Scale bars: 50 μm. (B,C) Recovery of ALR increased AMPK activation and reduced LDL uptake (n = 3 mice). Scale bars: 50 μm. Data are expressed as the mean ± SD for three independent experiments. **P < 0.01. Abbreviation: Adv-ALR, adenoviral-ALR.

studies strongly indicate that ALR-attenuated hepatic lipid accumulation is due, at least in part, to increasing mitochondrial β-oxidation. However, it is still unclear, apart from enhancement of fatty acid burnout offered by ALR, whether ALR itself could regulate the hepatic deposition of fatty acids, particularly cholesterol. Our present study demonstrates that the suppression of cholesterol uptake provided by ALR could be an alternative mechanism to reduce the lipid accumulation within hepatocytes. This conclusion is supported by the following observations: (1) increase in the hepatic lipid profile levels in MCD, CDE, or HFD *ALR*-lacking mice; (2) significant increase in the cholesterol levels in the livers of MCD, CDE, or HFD *ALR*-lacking mice and cultured ALR-lacking hepatocytes; (3) enhanced activation of SREBP2 and subsequent transcription of LDLR in *ALR*-lacking cells; and (4) negligible effect of ALR on the gene expression relevant to cholesterol synthesis, transformation, and efflux in mice.

Hepatic free cholesterol (FC) is a major lipotoxic molecule that promotes oxidative stress and liver damage, sensitizes to a more severe damage, and contributes to NASH pathogenesis.[10,35] Moreover, in patients and animal models of NASH, an increased amount of cholesterol, and in particular of FC, can be observed.[10,36] Extensive dysregulation of hepatic cholesterol homeostasis has been documented in NAFLD, leading to increased hepatic cholesterol levels.[6,9] This dysregulation likely occurs at multiple levels, such as increased hepatic cholesterol synthesis related to increased expression and activity of HMGCR,[37] increased hepatic levels of active SREBP2,[38] and increased uptake of cholesterol-rich-lipoproteins.[9] SREBP2 is an important transcription factor that regulates genes controlling both cholesterol synthesis and uptake events, including HMGCR and LDLR.[20] SREBP2 mRNA levels are higher in the liver of NASH patients.[38] In the present study, down-regulation of ALR-induced cholesterol accumulation was accompanied by the activation of SREBP2 and LDLR expression in the liver, but little with HMGCR alternation, suggesting clearly that the hepatic cholesterol accumulation caused by ALR deficiency is predominantly due to an increase in cholesterol uptake into hepatocytes, rather than its synthesis.

Previous studies have indicated that activation of AMPK could inhibit the expression and nuclear translocation of SREBP2.[32,39,40] Our current study also suggests that down-regulation of ALR may suppress AMPK activity, subsequently triggering SREBP2 and
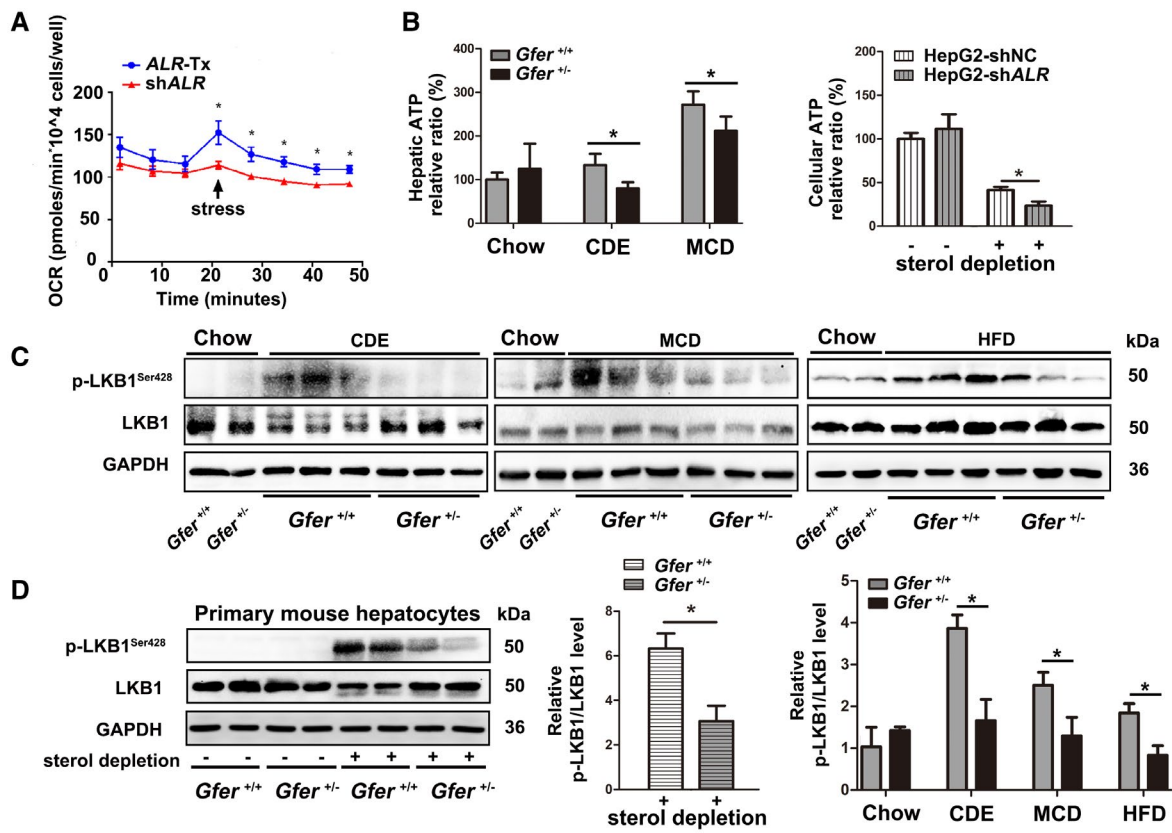
FIG. 9. Partial deletion of ALR impaired the mitochondrial functions. (A) OCR was detected by Seahorse technology. *ALR*-Tx and sh*ALR* HepG2 cells (1 × 10⁴) were stimulated (arrow) with oligomycin and carbonyl cyanide 4-(tri-fluoromethoxy) phenylhydrazone. (B) Hepatic (chow diet, n = 5 mice per group; CDE diet, n = 5 mice per group; MCD diet, n = 6 mice per group) and cellular ATP content were detected by CellTiter-Glo reagent (Promega, Madison, WI). (C,D) The phosphorylation of LKB1 in mice primary mouse hepatocytes was measured by western blot. In (A)-(D), data are expressed as the mean ± SD for three independent experiments, and each cell experiment was equipped with three multiple holes in each repetition. *$P < 0.05$.

phosphorylating AMPK-mediated target substrates (SREBP2, SREBP1c, and acetyl-coenzyme-A [CoA] carboxylase). Among this cascade of events, the regulation of AMPK activity plays a critical role.[41] SREBP1c is the main transcription factor to regulate *de novo* lipogenesis and enhances transcription of genes required for fatty acid synthesis.[42] Our previous study showed that ALR was able to suppress activation of SREBP1c, which would help the cells resist steatosis injury and apoptosis.[26] However, in this study we reveal that down-regulation of ALR, to some extent, did not elevate the levels of triglyceride and the expression and activation of SREBP1c in the liver significantly (Supporting Fig. S5). A robust explanation for these paradoxical observations could not be concluded from the current experimental data; however, we predict that this inconsistency might be due to differential responses to dietary challenge in *in vivo* models of steatohepatitis versus *in vitro* hepatocytes treated with sterol-free serum. The molecular mechanism underlying the selection of SBEBP2 over SREBP1 following down-regulation of ALR in hepatocytes is currently unknown. AMPK also phosphorylates and inactivates acetyl-CoA carboxylase 1/2 (ACC1/2), leading to a reduction in malonyl-CoA, which is an inhibitor of CPT1, the rate-limiting enzyme for mitochondrial fatty acid oxidation, and then increases fatty acid oxidation. This pathway may be consistent with previous reports demonstrating that ALR reduces lipid accumulation by increasing the activity of CPT1.[16,19,33] Our study did not detect the relationship between the activity of AMPK and the levels of free fatty acids and activity of CPT1 in *ALR*-lacking hepatocytes; therefore, these need further research.
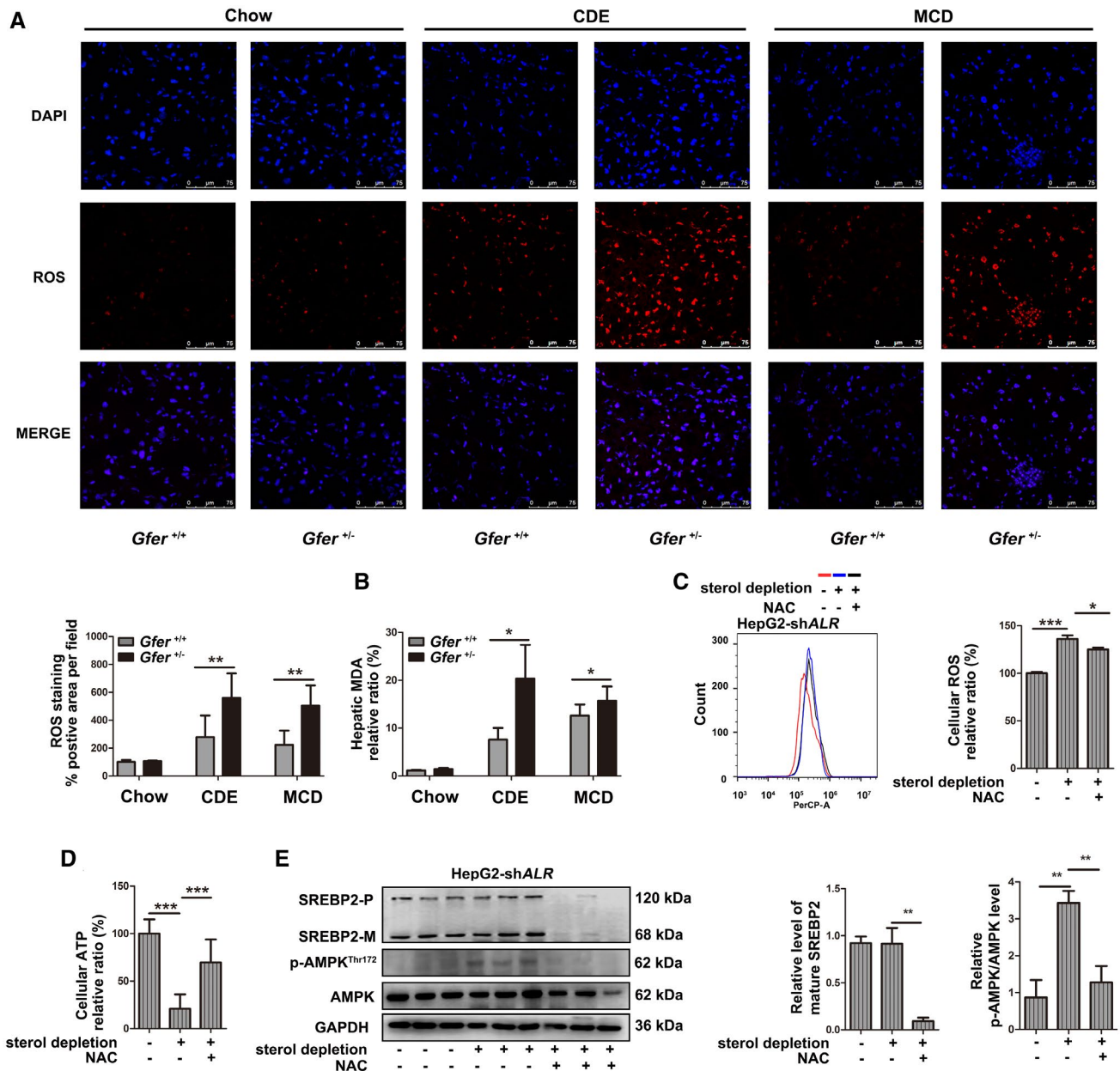
FIG. 10. Down-regulation of ALR expression increased the level of ROS and promoted SREBP2 maturation. (A) Detection of the localization and content of ROS in liver tissue by ROS probe for 30 minutes at 37℃. Relative fluorescence signals were evaluated at least three images per mouse by Imaging-Pro Plus (n = 5 mice per group). Scale bars: 75 μm. (B) After 4 weeks of CDE or MCD diet, hepatic MDA levels were measured (n = 5 mice per group). (C) Cellular ROS levels of HepG2 cells after LPDS treatment were detected. HepG2-sh*ALR* cells were pretreated with 5 mM NAC for 2 hours; after that, cells were lysed for the assay of cellular ROS (C) and ATP level (D). (E) Protein level of SREBP2-M and p-AMPK levels in NAC pretreated HepG2-sh*ALR* cells were measured. In (A)-(F), data are expressed as the mean ± SD for more than three independent experiments, with multiple holes in each repetition. *$P < 0.05$, **$P < 0.01$, ***$P < 0.001$.

The LKB1/AMPK pathway plays a crucial role in maintaining cellular metabolic homeostasis, especially in energy and lipid metabolism.[43] In light of ALR association with the LKB1/AMPK pathway, we first examined the energy status of the *ALR*-shRNA cells. Our results suggest that partial deletion of the *ALR* expression might also suppress the expression and activity of ATP synthase and cyclooxygenase 4 (data

not shown), leading to a remarkable decrease in ATP production. This observation is consistent with previous reports demonstrating that *ALR* deficiency could cause mitochondrial dysfunction, decrease in enzyme activity in the electron respiratory chain including ATP synthase subunit β, cytochrome c oxidase subunit 1, and nicotinamide adenine dinucleotide dehydrogenase β complex.[16,44] In agreement with our results, a decrease in liver ATP contents in humans with NAFLD, liver AMPK activity may actually be reduced.[30,31] In the liver, LKB1 is the major upstream kinase that can activate AMPK by phosphorylation.[45] As reported, LKB1 and AMPK could suppress the expression of various lipogenesis-related genes such as SREBP1 and fatty acid synthase, and ACC[46] inhibition of the LKB1/AMPK axis is believed to promote lipid and cholesterol synthesis as well as aggravating NAFLD conditions.[47] In this study, we found that partial deletion of the *ALR* expression could inhibit LKB1 phosphorylation, thereby inactivating AMPK-SREBP2-LDLR signaling delivery, which might in part account for the mechanism of ALR-alleviating cholesterol uptake.

Certainly, there are alternative mechanisms by which ALR exerts intermembrane space (IMS) molecular function. It had been previously reported that ALR interplays with Mia40 to constitute the mitochondria-specific disulfide relay system, which ensures adequate protein folding during import into IMS.[48] Mia40 oxidizes incoming proteins and is subsequently re-oxidized by ALR, which in turn transfers its electrons to cytochrome c, which is then acted upon by cytochrome c oxidase to convert oxygen to water.[49] The central role of ALR in this respiratory chain is to prevent the excessive generation of pathological levels of ROS, which has been taken as an example by the deletion of the *ALR* gene in *ALR*-floxed/floxed hepatocytes causing oxidative stress and mitochondrial damage.[16] Our current study also reveals that heterozygous deletion of ALR increases ROS levels in the livers of *Gfer*^{+/−} mice or *ALR*-shRNA hepatocytes and triggers the oxidative stress. Identically, a fresh report by Gandhi's lab demonstrates that ALR KO aggravates oxidative stress and promotes hepatic steatosis through up-regulation of miR-540 and inhibition of the key enzymes such as peroxisome proliferator–activated receptor α and CPT1.[50] Taking these results together, we predict that the SREBP2-LDLR pathway is also redox-sensitive. Although

ROS is known to regulate activity of both SREBP2 and AMPK,[32] knowledge of ROS to initiating AMPK-SREBP2 signaling in *ALR*-deficient hepatocytes is still lacking. Here we show that the activity of AMPK decreased after NAC was used; however, this decrease did not induce SREBP2 activation, suggesting that the redox-sensitive SREBP2-LDLR pathway is an AMPK-independent pattern, at least in the ALR-knockdown cells.

In conclusion, the hepatic accumulation of cholesterol caused by partial deletion of *ALR* is associated with SREBP2 activation triggered both by LKB1/AMPK signaling and ROS-induced stress.

REFERENCES

1) Schwimmer JB, Behling C, Newbury R, Deutsch R, Nievergelt C, Schork NJ, et al. Histopathology of pediatric in onalcoholic fatty liver disease. Hepatology 2005;42:641-649.

2) Younossi ZM, Otgonsuren M, Henry L, Venkatesan C, Mishra A, Erario M, et al. Association of nonalcoholic fatty liver disease (NAFLD) with hepatocellular carcinoma (HCC) in the United States from 2004 to 2009. Hepatology 2015;62:1723-1730.

3) Bugianesi E, Leone N, Vanni E, Marchesini G, Brunello F, Carucci P, et al. Expanding the natural history of nonalcoholic steatohepatitis: from cryptogenic cirrhosis to hepatocellular carcinoma. Gastroenterology 2002;123:134-140.

4) Mann JP, De Vito R, Mosca A, Alisi A, Armstrong MJ, Raponi M, et al. Portal inflammation is independently associated with fibrosis and metabolic syndrome in pediatric nonalcoholic fatty liver disease. Hepatology 2016;63:745-753.

5) Neuschwander-Tetri BA. Hepatic lipotoxicity and the pathogenesis of nonalcoholic steatohepatitis: the central role of nontriglyceride fatty acid metabolites. Hepatology 2010;52:774-788.

6) **Musso G**, **Gambino R**, Cassader M. Cholesterol metabolism and the pathogenesis of non-alcoholic steatohepatitis. Prog Lipid Res 2013;52:175-191.

7) Arguello G, Balboa E, Arrese M, Zanlungo S. Recent insights on the role of cholesterol in non-alcoholic fatty liver disease. Biochim Biophys Acta 2015;1852:1765-1778.

8) Hendrikx T, Walenbergh SM, Hofker MH, Shiri-Sverdlov R. Lysosomal cholesterol accumulation: driver on the road to inflammation during atherosclerosis and non-alcoholic steatohepatitis. Obes Rev 2014;15:424-433.

9) Min HK, Kapoor A, Fuchs M, Mirshahi F, Zhou H, Maher J, et al. Increased hepatic synthesis and dysregulation of cholesterol metabolism is associated with the severity of nonalcoholic fatty liver disease. Cell Metab 2012;15:665-674.

10) Ioannou GN. The role of cholesterol in the pathogenesis of NASH. Trends Endocrinol Metab 2016;27:84-95.

11) Dominguez-Perez M, Simoni-Nieves A, Rosales P, Nuno-Lambarri N, Rosas-Lemus M, Souza V, et al. Cholesterol burden in the liver induces mitochondrial dynamic changes and resistance to apoptosis. J Cell Physiol 2019;234:7213-7223.

12) Gan LT, Van Rooyen DM, Koina ME, McCuskey RS, Teoh NC, Farrell GC. Hepatocyte free cholesterol lipotoxicity results from JNK1-mediated mitochondrial injury and is HMGB1 and TLR4-dependent. J Hepatol 2014;61:1376-1384.

13) LaBrecque DR, Pesch LA. Preparation and partial characterization of hepatic regenerative stimulator substance (SS) from rat liver. J Physiol 1975;248:273-284.

14) Francavilla A, Hagiya M, Porter KA, Polimeno L, Ihara I, Starzl TE. Augmenter of liver regeneration: its place in the universe of hepatic growth factors. Hepatology 1994;20:747-757.

15) Nalesnik MA, Gandhi CR, Starzl TE. Augmenter of liver regeneration: a fundamental life protein. Hepatology 2017;66:266-270.

16) Weng J, Li W, Jia X, An W. Alleviation of ischemia-reperfusion injury in liver steatosis by augmenter of liver regeneration is attributed to antioxidation and preservation of mitochondria. Transplantation 2017;101:2340-2348.

17) Liu L, Xie P, Li W, Wu Y, An W. Augmenter of liver regeneration protects against ethanol-induced acute liver injury by promoting autophagy. Am J Pathol 2018;189:552-567.

18) Xiao W, Ren M, Zhang C, Li S, An W. Amelioration of nonalcoholic fatty liver disease by hepatic stimulator substance via preservation of carnitine palmitoyl transferase-1 activity. Am J Physiol Cell Physiol 2015;309:C215-C227.

19) Gandhi CR, Chaillet JR, Nalesnik MA, Kumar S, Dangi A, Demetris AJ, et al. Liver-specific deletion of augmenter of liver regeneration accelerates development of steatohepatitis and hepatocellular carcinoma in mice. Gastroenterology 2015;148:379-391.e374.

20) Horton JD, Goldstein JL, Brown MS. SREBPs: activators of the complete program of cholesterol and fatty acid synthesis in the liver. J Clin Invest 2002;109:1125-1131.

21) Han LH, Dong LY, Yu H, Sun GY, Wu Y, Gao J, et al. Deceleration of liver regeneration by knockdown of augmenter of liver regeneration gene is associated with impairment of mitochondrial DNA synthesis in mice. Am J Physiol Gastrointest Liver Physiol 2015;309:G112-G122.

22) Jia XW, Li ZW, Dong LY, Sun GY, Wang X, Gao J, et al. Lack of hepatic stimulator substance expression promotes hepatocellular carcinoma metastasis partly through ERK-activated epithelial-mesenchymal transition. Lab Invest 2018;98:871-882.

23) Denizeau F, Marion M, Chevalier G, Cote MG. Inability of chrysotile asbestos fibers to modulate the 2-acetylaminofluorene-induced UDS in primary cultures of rat hepatocytes. Mutat Res 1985;155:83-90.

24) Motazacker MM, Pirruccello J, Huijgen R, Do R, Gabriel S, Peter J, et al. Advances in genetics show the need for extending screening strategies for autosomal dominant hypercholesterolaemia. Eur Heart J 2012;33:1360-1366.

25) van der Windt GJ, Chang CH, Pearce EL. Measuring bioenergetics in T cells using a seahorse extracellular flux analyzer. Curr Protoc Immunol 2016;113:3.16B.1-3.16B.14.

26) Zhang J, Li Y, Jiang S, Yu H, An W. Enhanced endoplasmic reticulum SERCA activity by overexpression of hepatic stimulator substance gene prevents hepatic cells from ER stress-induced apoptosis. Am J Physiol Cell Physiol 2014;306:C279-C290.

27) Kleiner DE, Brunt EM, Van Natta M, Behling C, Contos MJ, Cummings OW, et al. Design and validation of a histological scoring system for nonalcoholic fatty liver disease. Hepatology 2005;41:1313-1321.

28) Wong J, Quinn CM, Brown AJ. SREBP-2 positively regulates transcription of the cholesterol efflux gene, ABCA1, by generating oxysterol ligands for LXR. Biochem J 2006;400:485-491.

29) Li Y, Xu S, Mihaylova MM, Zheng B, Hou X, Jiang B, et al. AMPK phosphorylates and inhibits SREBP activity to attenuate hepatic steatosis and atherosclerosis in diet-induced insulin-resistant mice. Cell Metab 2011;13:376-388.

30) Qiang X, Xu L, Zhang M, Zhang P, Wang Y, Wang Y, et al. Demethyleneberberine attenuates non-alcoholic fatty liver disease with activation of AMPK and inhibition of oxidative stress. Biochem Biophs Res Commun 2016;472:603-609.

31) Schmid AI, Szendroedi J, Chmelik M, Krssak M, Moser E, Roden M. Liver ATP synthesis is lower and relates to insulin sensitivity in patients with type 2 diabetes. Diabetes Care 2011;34:448-453.

32) Trewin AJ, Berry BJ, Wojtovich AP. Exercise and mitochondrial dynamics: keeping in shape with ROS and AMPK. Antioxidants (Basel) 2018;7. pii: E7.

33) Weiss TS, Lupke M, Ibrahim S, Buechler C, Lorenz J, Ruemmele P, et al. Attenuated lipotoxicity and apoptosis is linked to exogenous and endogenous augmenter of liver regeneration by different pathways. PLoS One 2017;12:e0184282.

34) Eaton S. Control of mitochondrial beta-oxidation flux. Prog Lipid Res 2002;41:197-239.

35) Dominguez-Perez M, Nuno-Lambarri N, Clavijo-Cornejo D, Luna-Lopez A, Souza V, Bucio L, et al. Hepatocyte growth factor reduces free cholesterol-mediated lipotoxicity in primary hepatocytes by countering oxidative stress. Oxid Med Cell Longevity 2016;2016:7960386.

36) Wouters K, van Bilsen M, van Gorp PJ, Bieghs V, Lutjohann D, Kerksiek A, et al. Intrahepatic cholesterol influences progression, inhibition and reversal of non-alcoholic steatohepatitis in hyperlipidemic mice. FEBS Lett 2010;584:1001-1005.

37) Simonen P, Kotronen A, Hallikainen M, Sevastianova K, Makkonen J, Hakkarainen A, et al. Cholesterol synthesis is increased and absorption decreased in non-alcoholic fatty liver disease independent of obesity. J Hepatol 2011;54:153-159.

38) Caballero F, Fernandez A, De Lacy AM, Fernandez-Checa JC, Caballeria J, Garcia-Ruiz C. Enhanced free cholesterol, SREBP-2 and StAR expression in human NASH. J Hepatol 2009;50:789-796.

39) Zhang M, Yuan Y, Wang Q, Li X, Men J, Lin M. The Chinese medicine Chai Hu Li Zhong Tang protects against non-alcoholic fatty liver disease by activating AMPKα. Biosci Rep 2018;38. pii: BSR20180644.

40) Lee JH, Jia Y, Thach TT, Han Y, Kim B, Wu C, et al. Hexacosanol reduces plasma and hepatic cholesterol by activation of AMP-activated protein kinase and suppression of sterol regulatory element-binding protein-2 in HepG2 and C57BL/6J mice. Nutr Res 2017;43:89-99.

41) Smith BK, Marcinko K, Desjardins EM, Lally JS, Ford RJ, Steinberg GR. Treatment of nonalcoholic fatty liver disease: role of AMPK. Am J Physiol Endocrinol Metab 2016;311:E730-E740.

42) Moon YA. The SCAP/SREBP pathway: a mediator of hepatic steatosis. Endocrinol Metab (Seoul) 2017;32:6-10.

43) Lin R, Elf S, Shan C, Kang HB, Ji Q, Zhou L, et al. 6-Phosphogluconate dehydrogenase links oxidative PPP, lipogenesis and tumour growth by inhibiting LKB1-AMPK signalling. Nat Cell Biol 2015;17:1484-1496.

44) Huang LL, Long RT, Jiang GP, Jiang X, Sun H, Guo H, et al. Augmenter of liver regeneration promotes mitochondrial biogenesis in renal ischemia-reperfusion injury. Apoptosis 2018;23:695-706.

45) Woods A, Johnstone SR, Dickerson K, Leiper FC, Fryer LG, Neumann D, et al. LKB1 is the upstream kinase in the AMP-activated protein kinase cascade. Curr Biol 2003;13:2004-2008.

46) Long JK, Dai W, Zheng YW, Zhao SP. miR-122 promotes hepatic lipogenesis via inhibiting the LKB1/AMPK pathway by targeting Sirt1 in non-alcoholic fatty liver disease. Mol Med 2019;25:26.

47) Sid V, Wu N, Sarna LK, Siow YL, House JD, O K. Folic acid supplementation during high-fat diet feeding restores AMPK activation via an AMP-LKB1-dependent mechanism. Am J Physiol Regul Integr Comp Physiol 2015;309:R1215-R1225.

48) Riemer J, Bulleid N, Herrmann JM. Disulfide formation in the ER and mitochondria: two solutions to a common process. Science 2009;324:1284-1287.

49) Banci L, Bertini I, Calderon V, Cefaro C, Ciofi-Baffoni S, Gallo A, et al. Molecular recognition and substrate mimicry drive the electron-transfer process between MIA40 and ALR. Proc Natl Acad Sci U S A 2011;108:4811-4816.

50) Kumar S, Rani R, Karns R, Gandhi CR. Augmenter of liver regeneration protein deficiency promotes hepatic steatosis by inducing oxidative stress and microRNA-540 expression. FASEB J 2019;33:3825-3840.

Author names in bold designate shared co-first authorship.

Supporting Information

Additional Supporting Information may be found at onlinelibrary.wiley.com/doi/10.1002/hep4.1532/suppinfo.